Numerical Study of Buoyancy Natural Convection in An Open Cavity

M. Almas[1,2,*]

[1]Department of Mechanical and Materials Engineering, Florida International University, Miami, FL 33199, USA

[2]Department of Marine engineering, King Abdulaziz University, 21589, Saudi Arabia

Abstract: Numerical study of buoyancy natural convection in open building rooms has been performed using Lattice Boltzmann Method (LBM). The right wall of the room is open, bottom is hot and the other walls are adiabatic. Numerical results are presented in terms of isotherms, streamlines and average Nusselt number to investigate the effects of various Rayleigh numbers and aspect ratios on heat transfer and fluid flow. It is concluded that as the aspect ratio decreases maximum rate of heat transfer happens when Rayleigh number increases.

Keywords: Natural convection, lattice boltzmann method, open room.

1. INTRODUCTION

Due to their numerous advantages, systems based on the heat transfer by natural convection are widely used in several engineering applications such as solar energy systems, electronic circuits cooling, air conditioning and natural ventilation in buildings. Heat transfer by natural convection in enclosures occurs in numerous applications and has been studied extensively in the literature [1-3]. In contrast, there is rather little work with open cavities, which constitute another important application area. Open cavities are encountered in various engineering systems, such as open cavity solar thermal receivers, electronic cooling devices, in buildings, passive systems, etc. Few numerical simulations in open cavities were reported for aspect ratio of unity [4-7]. On the other hand few research papers have been published on experimental studies of buoyant flow in open cavities [8-10]. Some basic approaches for analytical studies and also the study of natural convection and heat transfer in different building roofs is also considered extensively in engineering [11-24]. In this paper LBM is used to model the natural convection in a one side open building room (open cavity). Lattice Boltzmann Methods are in high pace development and have become a powerful method for simulation fluid flow and transport problems for single and multiphase flows [16, 17]. Most of the mentioned works (in cavities) investigated natural convection in cavities of aspect ratio of unity. The effect of systematic analysis of aspect ratio on the physics of flow and heat transfer is missing from the literature, which is worth being investigated. The velocity field and temperature profile are unknown at the opening boundary prior to solution. Such a boundary condition has been tested for LBM applications for the first time [18]. In present work, buoyancy natural convection in open building rooms has been performed using Lattice Boltzmann Method (LBM).

2. METHOD OF SOLUTION

Standard D2Q9 for both flow and temperature, LBM method is used in the present work [16]. The BGK approximation lattice Boltzmann equation without external forces can be written as,

$$f_i\left(X+c_i\Delta t,t+\Delta t\right)-f_i\left(X,t\right)=\Omega_i \tag{1}$$

where f_i are the particle distribution is defined for the finite set of the discrete particle velocity vectors c_i. The collision operator, Ω_i, on the right hand side of Eq. (1) uses the so-called Bhatangar-Gross-Krook (BGK) approximation [17]. For single time relaxation, the collision term Ω_i will be replaced by:

$$\Omega_i=\frac{f_i-f_i^{eq}}{\tau} \tag{2}$$

where $\tau\left(\tau=1/\omega_m\right)$ is the relaxation time and f_i^{eq} is the local equilibrium distribution function.

The equilibrium distribution can be formulated as [17]:

$$f_i^{eq}=\omega_i\rho\left[1+3\frac{c_i.u}{c^2}+\frac{9}{2}\frac{\left(c_i u\right)^2}{c^4}-\frac{3}{2}\frac{u u}{c^2}\right] \tag{3}$$

*Address correspondence to this author at the Department of Mechanical and Materials Engineering, Florida International University, Miami, FL 33199, USA; Tel: 7862103780; Fax: 00966126952437; E-mail: majidaaia@gmail.com

E-ISSN: 2409-5761/15

where u and ρ are the macroscopic velocity and density, respectively, and ω_i are the constant factors, for D2Q9 is given as,

$$\omega_i=\begin{cases} 4/9 & i=0, rest\ particle \\ 1/9 & i=1,3,5,7 \\ 1/36 & i=2,4,6,8 \end{cases} \tag{4}$$

The discrete velocities, c_i, for the D2Q9 (Figure **1**) are defined as follows:

$$\begin{aligned} &c_0=(0,0), c_k=c(\cos\theta_k, \sin\theta_k) \\ &\theta_k=(k-1)\pi/2 \ for\ k=1,2,3,4 \ \ c_k=c\sqrt{2}(\cos\theta_k, \sin\theta_k) \\ &\theta_k=(k-5)\pi/2+\pi/4 \ for\ k=5,6,7,8 \ \ c_k=c\sqrt{2}(\cos\theta_k, \sin\theta_k) \end{aligned} \tag{5}$$

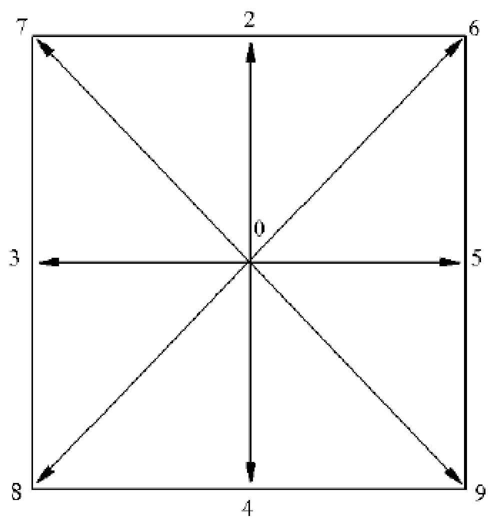

Figure 1: Nine-speed square lattice.

where $c=\Delta x/\Delta t$, Δx and Δt are the lattice space and the lattice time step size, respectively, which are set to unity. The basic hydrodynamic quantities, such as density ρ and velocity u, are obtained through moment summations in the velocity space:

$$\rho(X,t)=\sum_i f_i(X,t) \tag{6}$$

The macroscopic viscosity is determined by

$$\upsilon=\left[\tau-\frac{1}{2}\right]c_s^2\Delta t \tag{7}$$

where c_s is speed of sound and equal to $c_s/\sqrt{3}$. For scalar function (temperature), another distribution is defined,

$$g_k(\mathrm{x}+\Delta\mathrm{x}, \mathrm{t}+\Delta\mathrm{t})=g_i(x,t)[1-\omega_s]+\omega_s g_k^{eq}(x,t) \tag{8}$$

The equilibrium distribution function can be written as,

$$g_i^{eq}=\omega_k\phi(x,t)\left[1+\frac{\mathrm{c}_k\cdot\mathrm{u}}{c_s^{\ 2}}\right] \tag{9}$$

In which ω is different for momentum and scalar equations. For momentum,

$$\omega_m=\frac{1}{3\cdot\upsilon+0.5} \tag{10}$$

where υ is the kinematic viscosity and for the scalar

$$\omega_s=\frac{1}{2\cdot\alpha+0.5} \tag{11}$$

where α is the diffusion coefficient (thermal diffusion coefficient). Local Nusselt number is calculated as,

$$Nu_{local}=-\frac{\partial T}{\partial Y} \tag{12}$$

Nusselt number (Nu) is based on the length of the room (L). T stands for dimensionless temperature. Nusselt number is calculated by integrating Eq. (12) along the bottom length of the cavity.

For average Nusselt number we have

$$Nu_{ave}=\frac{Nu}{L} \tag{13}$$

The standard LBM consists of two steps, streaming and collision. D2Q9 is used to solve the velocity and temperature fields. The number of lattices used in x- and y-direction depends on the aspect ratio. At least 100 lattices are used in y-direction except for aspect ratio 0.5 in which the minimum number of lattices is taken as 200, and number of lattice in x-direction is aspect ratio multiplied by the number of lattices in the y-direction. The buoyancy force term is added as an extra source term to equation (1), as,

$$F_b=3\omega_k g\beta\triangle T \tag{14}$$

where g, β and $\triangle T$ are gravitational acceleration, thermal expansion coefficient and temperature difference.

3. BOUNDARY CONDITIONS

Figure **2** shows the configuration of natural convection [25-33] in an open room. The aspect ratio for the room is defined as $As=L/H$ varies from 0.5 to 3. No-slip boundary condition has been imposed on all

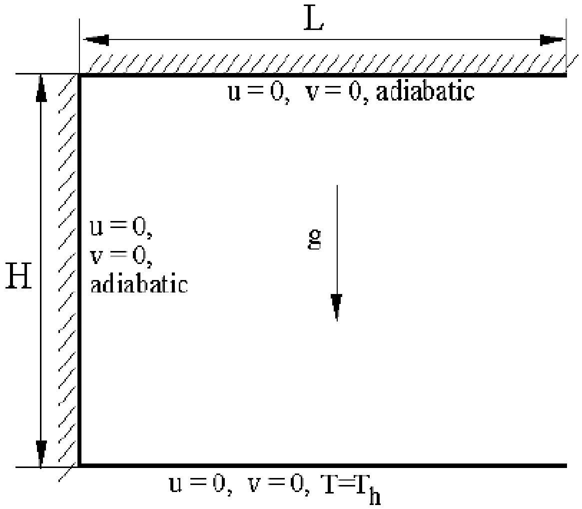

Figure 2: Configuration of natural convection in the open cavity.

the walls. The bottom wall is maintained at constant high temperature while the other walls are adiabatic and the east boundary is open. The boundary conditions have been implemented by using bounce back boundary condition for flow and temperature at all solid walls [18]. To handle the open boundary condition, a special treatment implemented as same the previous has been done [18].

4. RESULTS AND DISCUSSION

Natural convection in one side open building rooms is studied numerically using LBM [34]. The results obtained with the present code show good agreement with previous work [18] and finite volume method [35-] as presented in Table **1**. The simulations are carried out for different values of governing parameters which are Rayleigh number Ra and aspect ratio. Figures **3, 4, 5** and **6** show the streamlines (on the left) and isotherms (on the right) for $Ra = 10^3 - 10^6$ and aspect ratios of 0.5, 1.0, 2.0 and 3.0, respectively. The cold ambient fluid enters from the lower half portion of the room is heated by the bottom horizontal wall then moves upward due to the buoyancy forces and leaves from the upper half of the opening for all aspect ratios. Figure **3** shows streamlines and isotherms for aspect ratio of 0.5 for different Rayleigh numbers; at low Ra numbers ($10^3, 10^4$) streamlines are closer to each other near the bottom wall and by increasing the Ra number amassed streamlines move upward to the up wall due to strong buoyancy force; as it is obvious through streamlines and isotherms, for $Ra = 10^3$ and 10^4 some parts of the room are unventilated where the isotherms are not distributed thoroughly over the space and by increasing in Ra which result in higher heat transfer and stronger buoyancy force, the temperature gradient scatters in the space better and flow circulation inside the room gets more proper. Results for aspect ratio of 1.0 are displayed in Figure **4**. For $Ra = 10^3$ and 10^4 streamlines are equally spaced and when Ra grow streamlines are tilted upward at the upper corner of the closed end of the room due to strong buoyancy force. However, the strength of the buoyancy is not enough to form recirculation zone at the corner; at low Ra number isotherms show that the temperature gradient is almost constant along the room, where the isotherms are nearly equally spaced and for $Ra = 10^5$ flow is mainly stratified at the lower half of the room and the flow almost isothermal at the upper half of the room. Figure **5** demonstrates the results for aspect ratios of 2.0. For $Ra = 10^3$ there is also unventilated space which streamline grow as Ra increases and fluid flow get gradually stronger and develop to extend through the whole space (Figure **5**(**b**)) and for $Ra = 10^5$ the second cell forms due to increase in Ra and aspect ratio which like Figure **4**(**c**) streamlines are tilted upward at the upper corner of the closed end of the room due to strong buoyancy force and further increase of Ra to 10^6, increase buoyancy force and flow may form recirculation at the upper corner of the closed end of the room (Figure **5**(**c**)). Streamlines and isotherms in Figure **6** have similar trends like that of for aspect ratio 2.0 and for $Ra = 10^5$ (as aspect ratio increases to 3.0) flow becomes one dimensional as increasing aspect ratio for a given Ra decreases the rate of heat transfer up to the conduction limit. The rate of heat transfer is maximum for aspect ratio 0.5 and decreases as the

Table 1: Comparison of Mean Nusselt Number with Previous Works

Ra	Present	LBM [18]	FV ([18])
10^4	3.352	3.264	3.377
10^5	7.318	7.261	7.323
10^6	14.314	14.076	14.380

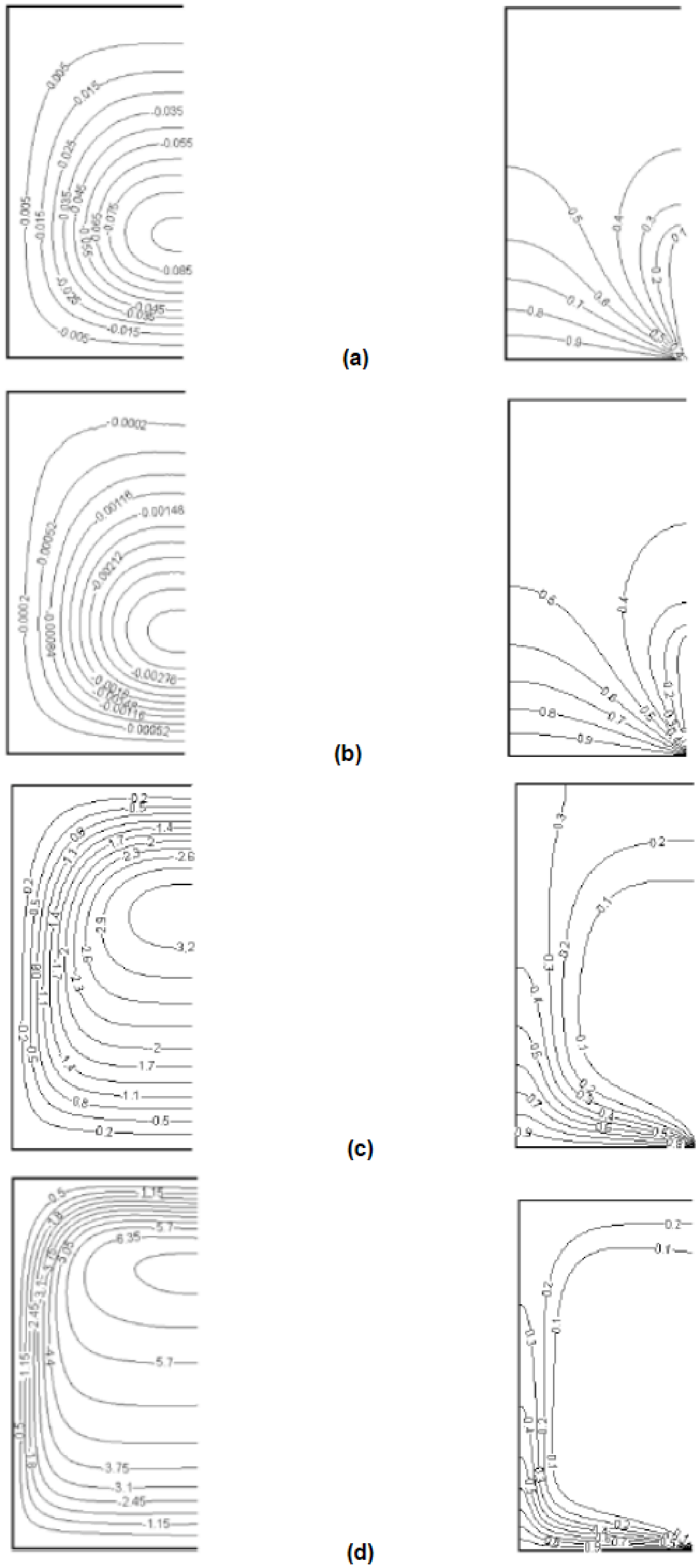

Figure 3: Streamlines (on the left) and Isotherms (on the right) for (a) $Ra = 10^3$, (b) $Ra = 10^4$, (c) $Ra = 10^5$, (d) $Ra = 10^6$ and aspect ratio of 0.5.

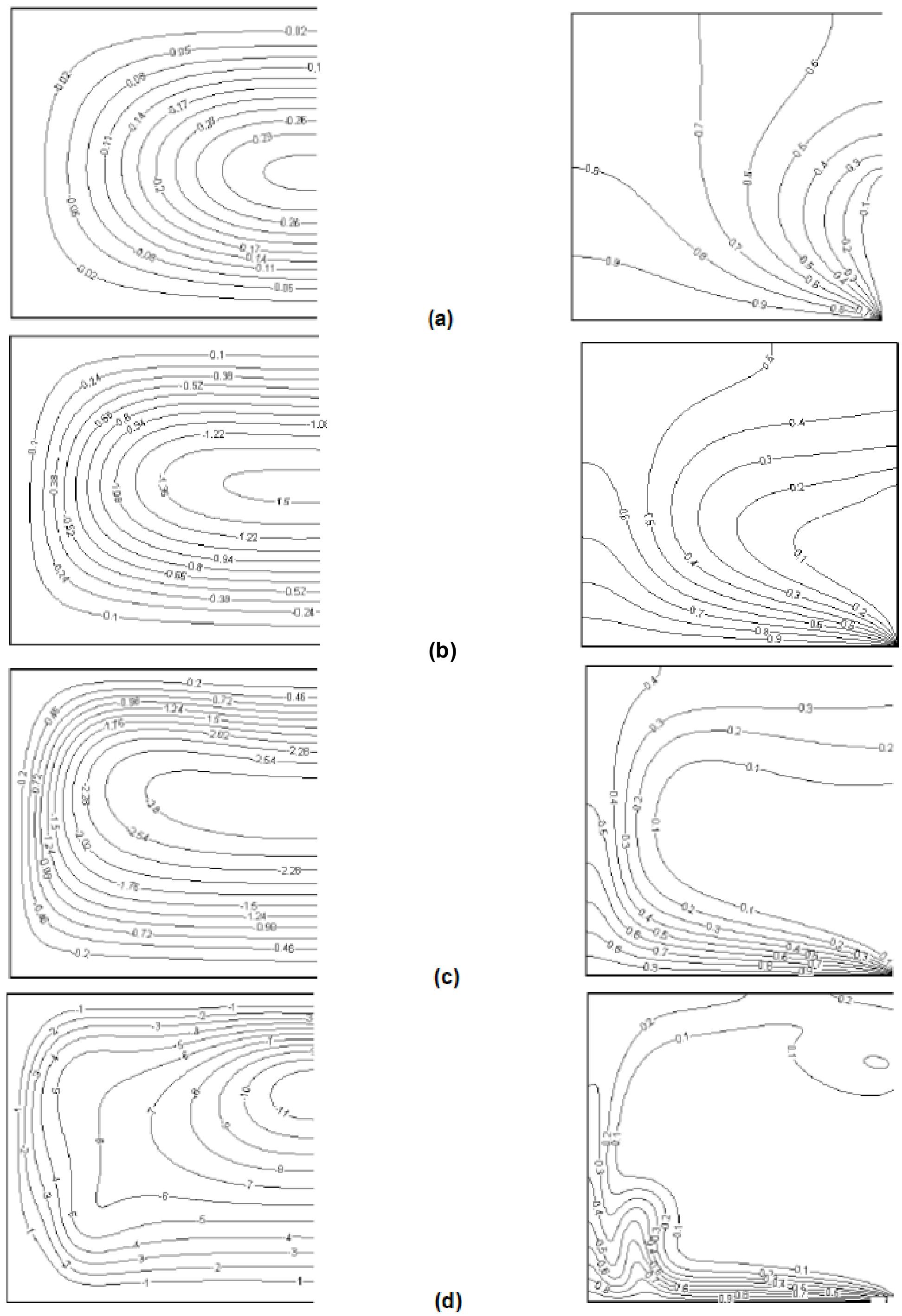

Figure 4: Streamlines (on the left) and Isotherms (on the right) for (a) $Ra = 10^3$, (b) $Ra = 10^4$, (c) $Ra = 10^5$, (d) $Ra = 10^6$ and aspect ratio of 1.0.

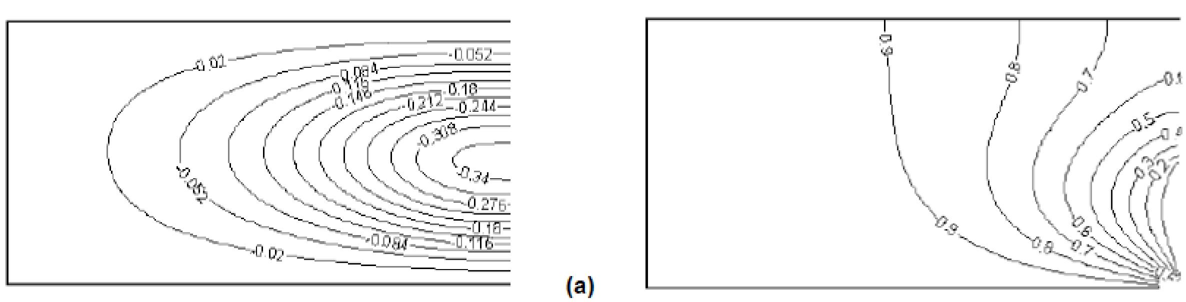

Figure 5 conti....

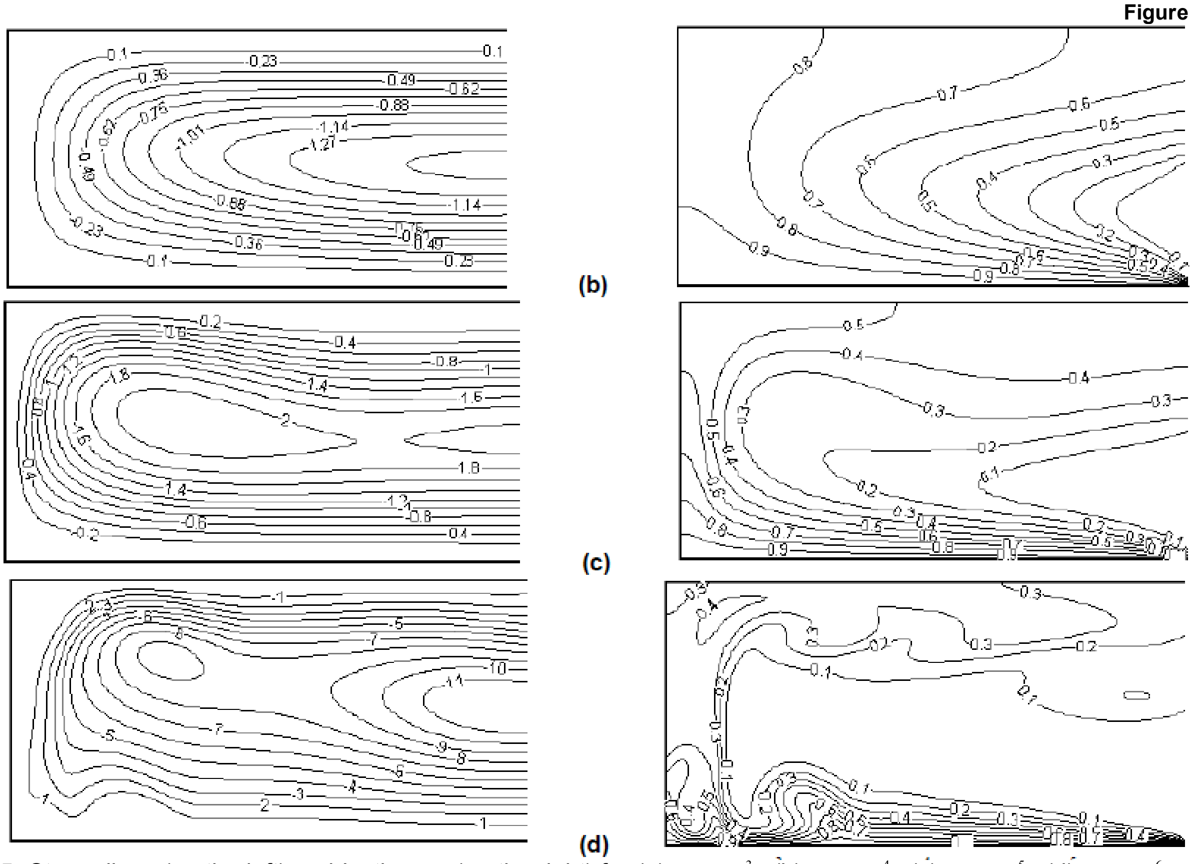

Figure 5: Streamlines (on the left) and Isotherms (on the right) for (a) $Ra = 10^3$, (b) $Ra = 10^4$, (c) $Ra = 10^5$, (d) $Ra = 10^6$ and aspect ratio of 2.0.

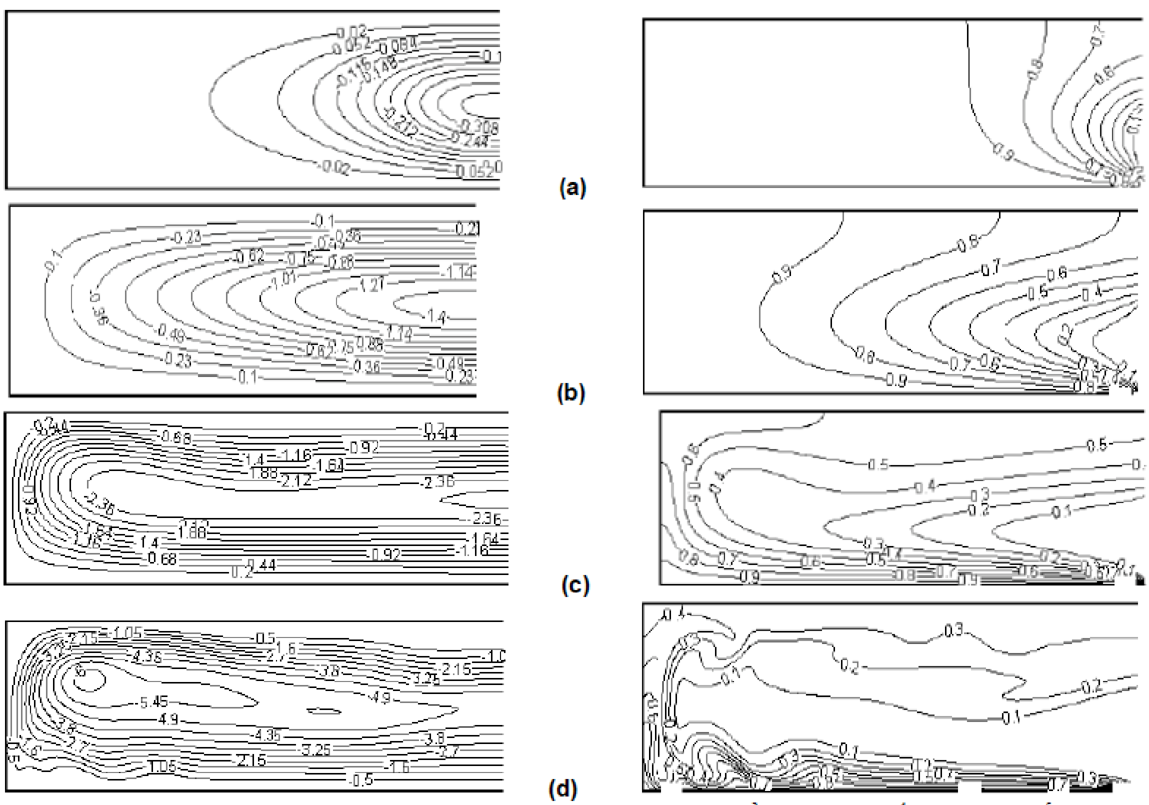

Figure 6: Streamlines (on the left) and Isotherms (on the right) for (**a**)Ra = 103, (**b**)Ra = 104, (**c**)Ra = 105, (**d**)Ra = 106 and aspect ratio of 3.0.

Table 2: Average Nusselt Number for Different Aspect Ratios and Rayleigh Numbers

Ra	Nu			
	As=0.5	As=1.0	As=2.0	As=3.0
10^3	3.797	4.150	4.326	4.334
10^4	3.734	5.948	7.659	8.126
10^5	5.813 ± 0.128	8.121	12.393	15.335
10^6	8.518 ± 0.297	12.383 ± 1.06	21.826 ± 3.471	27.459 ± 2.750
	Nu_{ave}			
10^3	7.594	4.150	2.163	1.445
10^4	7.468	5.948	3.830	2.708
10^5	11.626±0.256	8.121	6.197	5.112
10^6	17.036±0.594	12.383±1.06	10.913±1.736	9.153±0.916

aspect ratio increases due to hydraulic resistance, shear stress, added by the horizontal boundaries. The rate of heat transfer, Nusselt number is expected to reach conduction limit as the aspect ratio increases. Table **2** gives local Nusselt number for various aspect ratios at given Ra numbers; Nusselt increases as aspect ratios and Ra increase and maximum heat transfer happens for all aspect ratios at $Ra = 10^6$ in which the flow has an unsteady behaviour and the table also presents the results for average Nusselt number where the highest rate of heat transfer happens for aspect ratio 0.5 and this value decreases when aspect ratio grows.

5. CONCLUSION

Buoyancy driven flows in open building rooms are studied using LBM for a range of controlling parameters. Effects of various aspect ratios and Ra number on heat transfer and fluid flow is investigated. Numerical results shows that as the aspect ratio decreases, rate of heat transfer increases with growth of Rayleigh number. The results have been compared with previous works including finite volume method and as shown they are in excellent agreements. Results revealed that LBM is a very powerful numerical method in modelling fluid flow filed which has broad applications in engineering problems.

ACKNOWLEDGMENTS

The author would like to thank both the Saudi Arabian Cultural Mission in Washington D.C. and King Abdulaziz University in Jeddah, KSA for their support.

REFERENCES

[1] Randriazanamparany MA, Skouta A and Daguenet M. Numerical study of the transition toward chaos of twodimensional natural convection within a square cavity. Numeric Heat Transfer Part A: Appl 2005; 48(2): 127-147. http://dx.doi.org/10.1080/10407780490454386

[2] Dalal A, and Das MK. Natural convection in a rectangular cavity heated from below and uniformly cooled from the top and both sides. Numeric. Heat Transfer Part A: Appl 2006; 49 (3): 301-322. http://dx.doi.org/10.1080/10407780500343749

[3] Saeid NH and Yaacob Y. Natural convection in a square cavity with spatial side-wall temperature variation. Numeric Heat Transfer Part A: Appl 2006; 49(7): 683-697. http://dx.doi.org/10.1080/10407780500359943

[4] Penot F. Numerical calculation of two-dimensional natural convection in isothermal open cavities. Numeric Heat Transfer Part A: Appl 1982; 5(4): 421-437. http://dx.doi.org/10.1080/10407798208546995

[5] Chan Y and Tien C. A numerical study of two-dimensional natural convection in square open cavities. Numeric Heat Trans 1985; 8(1): 65-80. http://dx.doi.org/10.1080/10407798508552424

[6] Mohamad A. Natural convection in open cavities and slots. Numeric Heat Transfer Part A: Appl 1995; 27(6): 705-716. http://dx.doi.org/10.1080/10407789508913727

[7] Quere PL, Humphrey JA and Sherman FS. Numerical calculation of thermally driven two-dimensional unsteady laminar flow in cavities of rectangular cross section. Numeric Heat Trans 1981; 4(3): 249-283. http://dx.doi.org/10.1080/01495728108961792

[8] Chan Y and Tien C. Laminar natural convection in shallow open cavities. J Heat Trans 1986; 108(2): 305-309. http://dx.doi.org/10.1115/1.3246920

[9] Cha S and Choi K. An Interferometric Investigation of Open-Cavity Natural-Convection Heat Transfer. Int J Experiment Heat Trans 1989; 2(1): 27-40. http://dx.doi.org/10.1080/08916158908946352

[10] Hess C and Henze R. Experimental investigation of natural convection losses from open cavities. J heat trans 1984; 106(2): 333-338. http://dx.doi.org/10.1115/1.3246677

[11] Shao J, Liu J, Zhao J, Zhang W, Sun D and Fu Z. A novel method for full-scale measurement of the external convective heat transfer coefficient for building horizontal roof. Energy

Build 2009; 41(8): 840-847.
http://dx.doi.org/10.1016/j.enbuild.2009.03.005

[12] Clear R, Gartland L and Winkelmann F. An empirical correlation for the outside convective air-film coefficient for horizontal roofs. Energy Build 2003; 35(8): 797-811.
http://dx.doi.org/10.1016/S0378-7788(02)00240-2

[13] Biwole P, Woloszyn M and Pompeo C. Heat transfers in a double-skin roof ventilated by natural convection in summer time. Energy Build 2008; 40(8): 1487-1497.
http://dx.doi.org/10.1016/j.enbuild.2008.02.004

[14] Higishima A and Tanimoto J. Field measurements for estimating the convective heat transfer coefficient at building surface. Energy Build 2003; 38: 873-881.
http://dx.doi.org/10.1016/S0360-1323(03)00033-7

[15] Varol Y, Oztop HF and Varol A. Effects of thin fin on natural convection in porous triangular enclosures. Int J therm Scienc 2007; 46(10): 1033-1045.
http://dx.doi.org/10.1016/j.ijthermalsci.2006.11.001

[16] Mohamad A. Applied lattice Boltzmann method for transport phenomena, momentum. Heat and Mass Transfer Sure Print Calgary 2007.

[17] Succi S. The lattice Boltzmann equation: for fluid dynamics and beyond. Oxford university press 2001.

[18] Mohamad A, El-Ganaoui M and Bennacer R. Lattice Boltzmann simulation of natural convection in an open ended cavity. Int J Therm Scienc 2009; 48(10): 1870-1875.
http://dx.doi.org/10.1016/j.ijthermalsci.2009.02.004

[19] Qian Y, Ren D, Lai S and Chen S. Analytical approximations to nonlinear vibration of an electrostatically actuated microbeam. Commun Nonlin Sci Numer Simul 2012; 17(4): 1947-1955.
http://dx.doi.org/10.1016/j.cnsns.2011.09.018

[20] Ren ZF and Gui WK. He's frequency formulation for nonlinear oscillators using a golden mean location. Compu Math Appl 2001; 61(8): 1987-1990.
http://dx.doi.org/10.1016/j.camwa.2010.08.047

[21] Shou DH. The homotopy perturbation method for nonlinear oscillators. Compu Math Appl 2009; 58(11-12): 2456-2459.
http://dx.doi.org/10.1016/j.camwa.2009.03.034

[22] Zeng DQ. Nonlinear oscillator with discontinuity by the max–min approach. Chaos Solitons Fractals 2009; 42(5): 2885-2889.
http://dx.doi.org/10.1016/j.chaos.2009.04.029

[23] He JH. Hamiltonian approach to nonlinear oscillators Phys Lett A 2010; 374(23): 2312-2314.
http://dx.doi.org/10.1016/j.physleta.2010.03.064

[24] Xu L. Application of Hamiltonian approach to an oscillation of a mass attached to a stretched elastic wire. Math Comput Appl 2010; 15(5): 901-906.

[25] Ghasemi E, Soleimani S and Bayat M. Control Volume Based Finite Element Method Study of Nano-fluid Natural Convection Heat Transfer in an Enclosure Between a Circular and a Sinusoidal Cylinder 2013; 1-12.
http://dx.doi.org/10.1515/ijnsns-2012-0177

[26] Ghasemi E, Soleimani S and Bararnia H. Natural convection between a circular enclosure and an elliptic cylinder using Control Volume based Finite Element Method. Int Communicat Heat Mass Trans 2012; 39: 1035-1044.
http://dx.doi.org/10.1016/j.icheatmasstransfer.2012.06.016

[27] Bararnia H, Ghasemi E, Soleimani S, Baraei A and Ganji DD. HPM-Padé method on natural convection of Darcian fluid about a vertical full cone embedded in porous media. J Porous Media 2011; 14: 545-553.
http://dx.doi.org/10.1615/JPorMedia.v14.i6.80

[28] Soleimani KS, Ghasemi E and Bayat M. Mesh-free modeling of two-dimensional heat conduction between eccentric circular cylinders Thermal Physics; Int J Physic Scienc 2011; 6(16): 4044-4052.

[29] Soleimani S, Ganji DD, Gorji M, Bararnia H and Ghasemi E. Optimal location of a pair heat source-sink in an enclosed square cavity with natural convection through PSO algorithm. Int Communicat Heat Mass Trans 2011; 38: 652-658.
http://dx.doi.org/10.1016/j.icheatmasstransfer.2011.03.004

[30] Ghasemi E, Soleimani S, Bararnia H and Domairry G. Influence of Uniform Suction/Injection on Heat Transfer of MHD Hiemenz Flow in Porous Media. J Engineer Mech ASCE 2012; 138(1): 82-88.
http://dx.doi.org/10.1061/(ASCE)EM.1943-7889.0000301

[31] Ghasemi E, Bayat M and Bayat M. Visco-Elastic MHD flow of Walters liquid b fluid and heat transfer over a non-isothermal stretching sheet. Int J Phys Scienc 2011; 6(21): 5022-5039.

[32] Moghimi SM, Domairry G, Bararni H, Soleimani S and Ghasemi E. Numerical Study of Natural Convection in an Inclined L-shaped Porous Enclosure. Adv Theor Appl Mech 2012; 5: 237-245.

[33] Alinia M, Gorji M, Ganji DD, Soleimani S and Ghasemi E. Two-phase natural convection of SiO2-water Nano fluid in an inclined square enclosure. Transac B: Mech Engin 2014; 21(5): 1643-1654.

[34] Seyyedi SM, Soleimani S, Ghasemi E, Ganji DD, gorji M and Bararnia H. Numerical Investigation of Laminar Mixed Convection in a Cubic Cavity by MRT-LBM: Effects of the Sliding Direction. Numeric Heat Trans A 2013; 63: 285-304.
http://dx.doi.org/10.1080/10407782.2013.730456

[35] Ghasemi E, McEligot DM, Nolan K, Crepeau J, Siahpush A, Budwig RS and Tukohiro A. Effects of adverse and favorable pressure gradients on entropy generation in a transitional boundary layer region under the influence of freestream turbulence. Int J Heat Mass Transfer 2014; 77: 475-488.
http://dx.doi.org/10.1016/j.ijheatmasstransfer.2014.05.028

[36] Soleimani S, Ghasemi E and Almas MA. Effects of Pressure Gradients on Energy Dissipation Coefficient. J Advanc Therm Sci Res 2014; 1: 71-77.
http://dx.doi.org/10.15377/2409-5826.2014.01.02.6

[37] Ghasemi E, Soleimani S and Almas MA. Finite Element Simulation of Jet Combustor Using Local Extinction Approach within Eddy Dissipation Concep. J Advanc Therm Sci Res 2014; 1: 57-65.
http://dx.doi.org/10.15377/2409-5826.2014.01.02.4

[38] Bararnia H, Jalaal M, Ghasemi E, Soleimani S, Ganji DD, Mohammadi F. Numerical simulation of joule heating phenomenon using meshless RBF-DQ method. Int J Therm Sci 2010; 49: 2117-2127.
http://dx.doi.org/10.1016/j.ijthermalsci.2010.06.008

[39] Soleimani S, Jalaal M, Bararnia H, Ghasemi E, Ganji DD, Mohammadi F. Local RBF-DQ method for two-dimensional transient heat conduction problems. Int Communicat Heat Mass Trans 2010; 37: 411-1418.
http://dx.doi.org/10.1016/j.icheatmasstransfer.2010.06.033

[40] Jalaal M, Soleimani S, Domairry G, Ghasemi E, Bararnia H, Mohammadi F and Barari A. Numerical simulation of voltage electric field in complex geometries for different electrode arrangements using meshless local MQ-DQ method. J Electrostatics 2011; 69: 168-175.
http://dx.doi.org/10.1016/j.elstat.2011.03.005

[41] Taeibi RM, Ramezanizadeh M, Ganji DD, Darvan A, Ghasemi E, Soleimani S and Bararni H. Comparative study of large eddy simulation of film cooling using a dynamic global-coefficient subgrid scale eddy-viscosity model with RANS and Smagorinsky Modeling. Int Communicat Heat Mass Trans 2011; 38: 659-667.
http://dx.doi.org/10.1016/j.icheatmasstransfer.2011.02.002

[42] Ghasemi E, McEligot DM, Nolan K, Crepeau J, Tukohiro A, Budwig RS. Entropy generation in transitional boundary layer region under the influence of free stream turbulence using transitional RANS models and DNS. Int Comm Heat Mass Trans 2013; 41: 10-16.
http://dx.doi.org/10.1016/j.icheatmasstransfer.2012.11.005

[43] Ghasemi E, Soleimani S and Lin CX. Secondary reactions of turbulent reacting flows over a film-cooled surface. Int Communicate Heat Mass Trans 2014; 55: 93-101. http://dx.doi.org/10.1016/j.icheatmasstransfer.2014.04.007

[44] Ghasemi E, Soleimani S and Lin CX. RANS simulation of methane-air burner using local extinction approach within eddy dissipation concept by Open FOAM. Int Communicate Heat Mass Trans 2014; 54: 96-102. http://dx.doi.org/10.1016/j.icheatmasstransfer.2014.03.006

Received on 31-03-2015 Accepted on 16-04-2015 Published on 14-12-2015

DOI: http://dx.doi.org/10.15377/2409-5761.2015.02.02.1